JOURNAL OF COMPUTATIONAL PHYSICS 91, 174–196 (1990)

A Two-Dimensional Adaptive Pseudo-Spectral Method*

A. BAYLISS, R. KUSKE, AND B. J. MATKOWSKY

Department of Engineering Sciences and Applied Mathematics, Northwestern University, Evanston, Illinois 60208

Received April 25, 1989; revised October 27, 1989

We develop a two-dimensional adaptive pseudo-spectral procedure which is capable of improving the approximation of functions which are rapidly varying in two dimensions. The method is based on introducing two-dimensional coordinate transformations chosen to minimize certain functionals of the solution to be approximated. The method is illustrated by numerical computation of the solutions to a system of reaction diffusion equations modeling the gasless combustion of a solid fuel. Spatio-temporal patterns are computed as a parameter μ, related to the activation energy, is increased above a critical value μ_c. The spatial patterns are characterized by a very rapid variation in the direction of the axis of the cylinder, together with a standing wave pattern in the direction of the azimuthal angle ψ. For small values of $\mu - \mu_c$ the solutions exhibit a nearly sinusoidal dependence in both time and ψ. As μ is increased further relaxation oscillations in both time and ψ occur. Beyond a critical value of μ stable time-periodic solutions are no longer found and the solution exhibits a quasi-periodic time dependence.

INTRODUCTION

In this paper we present an adaptive pseudo-spectral procedure for two-dimensional problems. The method is an extension of our earlier method [1, 7] which was developed for problems which are either posed in one dimension or can be treated by a Cartesian product adaptive procedure. The method relies on the introduction of two-dimensional (non-Cartesian product) coordinate transformations which are obtained from minimizing certain functionals monitoring the spectral interpolation error. The method will be illustrated by the calculation of pulsating cellular flames for problems in solid fuel combustion.

The Chebyshev pseudo-spectral method has found applications in a wide range of problems in the general area of fluid dynamics (see [8] and the references contained therein). It is known that pseudo-spectral methods are well suited for the approximation of functions which are smooth and do not exhibit localized regions of rapid variation [8, 12]. For functions exhibiting regions of rapid variation, oscillations can develop which can lead to inaccuracies and nonlinear instabilities [11]. Filtering and post-processing of the solution have been used with the

* This research was supported in part by DOE Grant DEFG02-87ER-25027, Contract W-31-109-Eng-38, and NSF Grants DMS 87-01543 and ASC 87-19583.

0021-9991/90 $3.00

Chebyshev pseudo-spectral method in the calculation of weak solutions of conservation laws [11]. These methods have been applied to problems in two dimensions; however, their applicability to problems with strongly (e.g., exponentially) nonlinear reaction terms such as occur in many combustion problems, has not been shown.

In many combustion problems diffusion is present so that shocks or weak solutions generally do not occur. It is typical of combustion problems, however, that the activation energies are large so that the chemical reaction terms are important only in a narrow region called the reaction zone. Ahead of the reaction zone the temperature is too cold to sustain the reaction while beyond the reaction zone the fuel has been consumed so that the reaction can not occur. As a result the solutions of typical combustion problems, while smooth, generally have localized regions where the variation is very rapid. In addition, the reaction terms often depend exponentially on the pointwise value of the solution, which makes filtering type procedures unattractive. An alternative is to introduce coordinate transformations so that in the transformed coordinate the error in the pseudo-spectral approximation is reduced. In effect, the transformations tend to expand the reaction zone, thus resulting in functions with a more gradual spatial variation. Generally the location of the reaction zone is not known in advance and therefore appropriate coordinate transformations must be obtained adaptively from the computed solution.

In [1, 7, 13] an adaptive pseudo-spectral method was introduced. The method was effective in improving the calculation of a variety of problems in both gaseous and solid fuel combustion. The method was based on introducing a family of coordinate transformations depending on a small number of parameters. A particular coordinate system was chosen dynamically by minimizing a certain integral functional which was an upper bound for the spectral interpolation error in some norm. In [1, 13] the second Sobolev norm of some component of the solution was minimized. This provided a bound on the L_2 norm of the spectral interpolation error. The method was illustrated by examples from solid fuel combustion and shown to be effective in improving the resolution of rapidly varying functions.

In [7] a different functional was considered. This functional was derived directly from the Chebyshev expansion of an arbitrary function and was shown to be an upper bound for the maximum norm of the spectral interpolation error. The use of this functional was illustrated by numerical computations of pulsating axisymmetric solutions for certain problems of gaseous combustion.

For planar and/or axisymmetric problems there is no spatial structure transverse to the reaction zone. In this case the one-dimensional transformations considered in [1, 7] were sufficient to provide adequate resolution of the reaction zone. There are however, many problems where there is spatial structure transverse to the reaction zone. In these problems cells form, leading to a periodic variation in the location of the reaction zone as the transverse coordinate is varied. The transverse coordinate may be an angular coordinate in either a cylindrical or polar coordinate system. Cellular solutions have been found for problems in solid and gaseous fuel combustion. These cellular solutions can either be time independent (stationary

cells), can propagate with a uniform velocity, or they can have a temporal structure. In the latter case the temporal structure is often a periodic (in time) pulsation and the solutions are referred to as pulsating cellular flames. In this paper we illustrate the numerical method by the computation of pulsating cellular flames for problems in solid fuel combustion. Analysis of these solutions can be found in [10, 19]. Typically in pulsating cellular flames, the location of the reaction zone varies in both space and time. The spatio-temporal variation can be described as a standing wave with fixed nodes or a traveling wave propagating along the reaction zone, (which itself may be propagating into the fresh fuel mixture).

The numerical method presented in [1, 7] is not directly applicable to cellular flames because of the use of one-dimensional mappings. The mappings, in effect, are designed to spread out regions of rapid variation normal to the reaction zone. When the location of the reaction zone depends on an angular coordinate, no one-dimensional mapping will be optimal. In addition there is no natural single functional which monitors the spectral interpolation error for each angular direction. In [5, 7] the one-dimensional procedure was used to compute stationary cellular flames for a model of gaseous combustion in polar coordinates. In this case the one-dimensional mapping was chosen by minimizing the sum of the computed functionals in each direction.

The results in [5] demonstrated that although the use of a one-dimensional transformation can be effective, this method becomes less effective for large amplitude cells where there is a significant angular variation in the location of the reaction zone. In this case sufficiently many collocation points must be used to adequately resolve the reaction zone in each angular direction. The use of Cartesian product transformations will not generally account for an angular variation in the location of the reaction zone. Non-product adaptive pseudo-spectral procedure have not been previously developed. Such a procedure is presented here.

One approach is to use a general two-dimensional transformation. However, this is difficult to implement in the context of the Chebyshev pseudo-spectral method. In our adaptive procedure, we work with explicitly defined mapping functions and for efficiency we restrict our attention to mappings which are explicitly invertible. In addition, the most general two-dimensional mappings may not be required for typical combustion problems where the major angular variation is in the location of the reaction zone, whereas the very sharp gradients due to the reaction terms occur primarily in the direction normal to the reaction zone. Often this direction has only a weak dependence on the angular variable.

In the method presented here we employ a family of one-dimensional transformations in the direction normal to the reaction zone (axial direction for the cylindrical geometry considered in the examples). These transformations depend on a small number of parameters which are obtained by minimizing an appropriate functional of the solution. The minimization is carried out in each angular direction and the parameters of the transformation determined as a function of the angular variable. This method has been implemented and used to study pulsating cellular solutions in gasless solid fuel combustion.

In this type of combustion, the chemical reaction occurs directly in the solid without the formation of a gaseous phase (although a liquid phase can occur). This method is currently being investigated as a new and more efficient method of synthesizing certain ceramic and metallic alloys. The synthesis occurs by the propagation of a high temperature combustion wave through the sample which converts reactants into products. This process is referred to as the SHS process (for "self-propagating high temperature synthesis") [15, 22].

It has been observed that the combustion wave does not always propagate with a uniform velocity. Planar pulsating modes of combustion have been observed, where the planar combustion wave propagates with an oscillatory velocity. These modes are identified by a periodic planar striation in the sample. Nonplanar modes of combustion have also been observed. In spin combustion, hot spots (luminous points) propagate in a helical fashion around the sample. Multiple point combustion is characterized by the appearance, disappearance, and reappearance of one or more luminous points on the surface of the sample. In addition, for certain mixtures, combustion occurs only on the surface while for other mixtures the burning occurs throughout the entire sample. Finally, it has been observed that often the temperature is sufficiently high so that one or more of the reactants melts prior to reaction [14–17, 22, 23].

Analytical models, based on an infinite activation energy model for the reaction term, have been extensively investigated [18–21, 25]. Planar pulsating combustion has been identified as due to a Hopf bifurcation occurring when a parameter μ, related to the non-dimensional activation energy and the ratio of the temperature of the burned and unburned material, exceeds a certain value [21]. This problem has also been studied numerically [1, 3, 4]. Numerical computations have found a period doubling secondary bifurcation occurring when μ is increased. In [4] it was shown that upon further increasing μ the solution returned to single periodicity. In [3] it was shown that multiple windows of period doubled behavior could exist as μ was increased. Beyond a certain point it was found that periodic solutions could no longer be computed and the solution exhibited intermittency, with long laminar regions interrupted by occasional bursts until apparently fully chaotic solutions were computed.

Spin combustion and multiple point combustion have been identified with traveling wave and standing wave solutions emanating from Hopf bifurcations corresponding to non-planar solutions [10, 19]. Both traveling and standing wave solution branches can be shown to exist, but the stability of each branch depends on the details of the particular problem being analyzed. In addition, quasi-periodic modes of propagation have been identified as due to degenerate and secondary bifurcation points [20]. Numerical computations of an example of spin combustion were presented in [22]; however, the behavior of the solution along such pulsating cellular branches has not been studied. Numerical examples of both multiple point combustion and spin combustion have been presented in [2, 6]. These results are extended here as an application of the numerical method. Specifically, we will demonstrate the evolution of the increasingly relaxational character of the solution

along a standing wave solution branch. The computations will also demonstrate a transition to a branch of apparently quasi-periodic solutions.

The remainder of this paper is organized as follows. In Section 2 we describe the two-dimensional pseudo-spectral adaptive procedure used in our calculations. In Section 3 we describe a model of surface combustion which accounts for the effects of melting and which is used in our calculations. In Section 4 we describe the results of computations employing the method.

2. Numerical Method

We consider problems which exhibit non-periodic behavior in one direction (x) and are periodic in the transverse direction (y). The numerical method is based on the Chebyshev pseudo-spectral method in the x direction and the Fourier pseudo-spectral method in the y direction. Extensive discussions of these methods can be found in [8, 12]. We assume familiarity with the Fourier pseudo-spectral method. Since the Chebyshev pseudo-spectral method is central to the adaptive procedure in our problems, we give a brief description.

Consider the heat equation

$$u_t = u_{xx}. \tag{2.1}$$

In the Chebyshev pseudo-spectral method the equation is solved at a set of J collocation points x_j ($j = 1, ..., J$). The solution at x_j is denoted by u_j. The usual collocation points are the Gauss–Lobatto points, i.e., the extrema of the Jth Chebyshev polynomial $T_J = \cos(J \cos^{-1} x)$,

$$x_j = \cos j\pi/J. \tag{2.2}$$

For the purposes of computing the spatial derivatives the solution u to (2.1) is approximated by a sum of Chebyshev polynomials

$$u_J = \sum_{j=0}^{J} a_j T_j(x). \tag{2.3}$$

The expansion coefficients a_j in (2.3) are obtained from collocation; i.e., we require that (2.3) satisfy (2.1) at the points (2.2). Spatial derivatives are computed by explicitly differentiating the finite series (2.3) and evaluating the result at x_j. The function values are then found from integrating the resulting set of ordinary differential equations in time. Further details of the method can be found in [8, 12].

It is known that oscillations can arise in applying this method to functions exhibiting rapid spatial variation over narrow regions [11]. In certain circumstances these oscillations can be removed by suitable post-processing of the solution. However, in combustion problems the solution is influenced by exponentially nonlinear reaction terms. These reaction terms are sensitive to the pointwise value of

the solution. Oscillations can result in an incorrect description of the dynamics and sometimes lead to instabilities in the computation. In combustion problems of the type considered here the solutions are in fact smooth in all regions of space and the oscillations can be removed by increasing the number of collocation points.

A more efficient approach is to introduce an adaptive procedure to enhance the accuracy of the computation. Such a procedure was introduced in [1] and also in [13]. In this procedure a family of coordinate transformations depending on a small number of parameters

$$x = q(s, \boldsymbol{\alpha}) \tag{2.4}$$

is introduced. Here $\boldsymbol{\alpha}$ denotes a parameter vector which is to be determined. Equation (2.4) describes a change of variables which can be applied to equation (2.1). The Chebyshev pseudo-spectral method can then be applied to the transformed equation

$$u_t = \frac{u_{ss}}{q'^2} - \frac{u_s q''}{q'^3}. \tag{2.5}$$

The parameters $\boldsymbol{\alpha}$ are chosen so that in the new coordinte system some bound on the spectral interpolation error is minimized. These bounds are typically functionals of the solution involving integrals of derivatives of the solution. Two examples which have been considered are

$$I(u) = \int_{-1}^{1} ds \frac{(u_{ss}^2 + u_s + u^2)}{\sqrt{1-s^2}} ds \tag{2.6}$$

$$\tilde{I}(u) = \int_{-1}^{1} \frac{ds}{\sqrt{1-s^2}} \left[\left(\sqrt{1-s^2} \frac{d}{ds} \right)^2 u \right]^2. \tag{2.7}$$

Numerical examples presented in [7] demonstrated that (2.7) is a more effective estimator of the spectral interpolation error, particularly for problems where the reaction zone occurs in the interior of the domain. However, for problems where the region of rapid variation occurs near the boundary, as is the case here, we have found that the use of either (2.6) or (2.7) leads to similar results. The computations presented here were obtained by minimizing (2.6).

The effect of the adaptive procedure is to change the basis functions in the original coordinate (x), so as to better resolve the solution. In the computations, the transformed equation (2.5) is solved using the Chebyshev pseudo-spectral method. The functionals are computed in the general coordinate system determined from (2.4). The parameter vector $\boldsymbol{\alpha}$ is then chosen as a minimizer of the resulting functional. The solution is then interpolated to the newly chosen coordinate system by computing the global Chebyshev interpolant and the calculation then continued until a new search for a coordinate system is triggered. In [1, 4] a planar version

of the solid combustion problem considered below was solved and the one-parameter family of coordinate transformations

$$q(s, \alpha) = \frac{4}{\pi} \tan^{-1} \alpha \tan\left(\frac{\pi}{4}(s-1)\right) + 1 \tag{2.8}$$

was found to be effective in computing very rapidly varying solutions.

This method is effective in adaptively stretching the reaction zone for planar problems. We now consider the two-dimensional model problem

$$u_t = u_{xx} + u_{yy}. \tag{2.9}$$

In the applications presented below y will be an angular variable and the location of the reaction zone will have an angular dependence. The method described above can enhance the resolution of the reaction zone for one angle but may not provide adequate resolution of the reaction zone at other angles. In addition, there is no natural way to select a preferred angle to apply the procedure described above or to create appropriate functionals.

Since regions of rapid variation still occur primarily in the x direction we now consider the two-dimensional family of mappings

$$\begin{aligned} x &= q(s, \boldsymbol{\alpha}(\tau)) \\ y &= \tau \end{aligned} \tag{2.10}$$

applied to (2.9). The mappings in this family have the flexibility to stretch the reaction zone (or to alter the basis functions) differently for different values y. The mappings have the additional advantage of being explicitly invertible provided this is true for the one-dimensional mapping. The Jacobian of the mapping can also be explicitly computed. Finally the functionals (2.6) and (2.7) provide mathematically sound error bounds to be minimized for each fixed value of y.

In our method, (2.6) is computed for each value of the angular coordinate y. For each such value of y, (2.6) is minimized and the minimizer computed. The function $\boldsymbol{\alpha}(y)$ is then computed via Fourier interpolation. Typically the resulting function is filtered to remove high frequency modes which can enter due to the minimization. The equation is then transformed by the mapping (2.10), to

$$u_t = (u_s s_x)_s s_x + (u_s s_y)_s s_y + 2u_{ts} s_y + u_{\tau\tau} + u_s s_{y\tau}. \tag{2.11}$$

In (2.11) the first two terms are kept in conservation form which is the way they are treated in our computer program. In deriving (2.11) we have made use of special properties of the mapping (2.10). The terms s_x, s_y, and $s_{y\tau}$ can be evaluated as functions of s and τ by differentiating (2.10). We introduce the notation $q_1 = \partial q/\partial s$, $q_2 = \partial q/\partial \tau$ with a similar notation for higher derivatives. It can then be easily seen that

$$s_x = \frac{1}{q_1}, \qquad s_y = -\frac{q_1}{q_2}, \qquad s_{y\tau} = \frac{-q_{12}q_2 + q_1 q_{22}}{q_2^2}.$$

We note that the computation of these terms involves computing $d\alpha/d\tau$. This is done using a Fourier pseudo-spectral method. The transformed equation (2.10) is then solved using a Chebyshev pseudo-spectral method in s and a Fourier pseudo-spectral method in τ.

The computational overhead associated with the minimization is generally not large. The transformed equation (2.11) differs from the model equation (2.9) in two important respects: there is an angle dependent coefficient multiplying the second s-derivative term and mixed derivatives now appear in the equation. These additional terms can effect the efficiency of time differencing schemes which we now discuss.

It is typical in pulsating combustion problems that the solution exhibits regions of very rapid temporal oscillations. These solutions take on the character of relaxation oscillations, examples of which are presented in [1, 3, 4]. In order to accurately compute these solutions, small timesteps are generally required. Consequently only the explicit timestep restriction due to the second s-derivative terms (the first two terms on the right-hand side of (2.11)) is limiting and we use a semi-implicit integration method in time. In our computations for the model described below, the analogues of the first two terms are treated implicitly and the other terms are treated explicitly.

The transformed equation (2.11) has variable coefficients multiplying these terms while in the untransformed equation (2.9), the coefficients are independent of t and y, so that the implicit equations can be solved by factoring a constant matrix. In (2.11) this would require a different matrix to be factored for each value of τ (i.e., each angle). In order to reduce the computer storage requirements we use an iterative method to solve the linear equations resulting from the semi-implicit time differencing. The mixed derivative term in (2.11) requires some additional computation and could force an additional timestep restriction.

Therefore the major computational costs associated with the two-dimensional adaptive procedure are (i) the requirement for an iterative solution method to solve the linear equations obtained from the implicit time differencing, (ii) the computation of the mixed derivatives, and (iii) a possible reduction of the timestep due to the mixed derivative terms. For any particular problem these costs must be balanced against the reduction in collocation points that can be obtained by transforming the coordinate system differently for each value of the transverse coordinate. In the applications considered here the problem is transformed to a nonseparable coordinate system, so that both variable coefficients and mixed derivatives are already present (see below). In this case the added computational expense of the two-dimensional adaptive procedure is minimal. Similar considerations hold for many other problems in fluid dynamics, combustion, and other areas of science and engineering and the numerical method introduced here should enhance the efficiency of pseudo-spectral computations for these problems.

Cellular solutions also occur in problems of gaseous combustion [5, 7]. In the models that we have solved previously there are constant diffusion coefficients. In this case the efficiency of the two-dimensional procedure depends on the amplitude

of the cells. For moderate amplitude cells such as those considered in [5, 7] a one-dimensional adaptive procedure, together with the high order accuracy of the Chebychev pseudo-spectral method is sufficient to adequately resolve the solution. For larger amplitude cells the situation is analogous to the solid combustion problem considered here and, in this case, the benefits of reducing the number of collocation points would seem to outweigh the cost of the iterative solution of the semi-implicit scheme.

Many of the features of this method are well suited to parallel computer architectures. For example, the iterative solution to the system of linear equations obtained from the temporal differencing can be parallelized in the transverse direction. We have found that the convergence rate of the iterative method is relatively insensitive to the transverse variable. In our current implementation of the method we employ a fixed number of iterations (generally one or two) for each angular variable. Thus the computational cost of the solution of the linear equations is independent of the transverse variable, providing potentially optimal load balancing among multiple processors. Another facet of the method which is potentially parallelizable is the minimization of the functional (either (2.6) or (2.7)).

3. Solid Combustion Model

We employ a model similar to the model employed in [21]. The model accounts for melting of a deficent component as described in [18]. We consider irreversible, one-step Arrhenius kinetics and assume that there is no diffusion of mass in either the solid or liquid phase. We denote by $\sim$ a dimensional quantity. The equations of the model are given by

$$\frac{\partial \tilde{T}}{\partial \tilde{t}} = \tilde{\lambda} \nabla^2 \tilde{T} + \begin{pmatrix} \tilde{\beta} \\ \alpha(\tilde{\beta} + \tilde{\gamma}) \end{pmatrix} \tilde{A} \tilde{Y} \exp(-\tilde{E}/\tilde{R}\tilde{T})$$

$$\frac{\partial \tilde{Y}}{\partial \tilde{t}} = -\begin{pmatrix} 1 \\ \alpha \end{pmatrix} \tilde{A} \tilde{Y} \exp(-\tilde{E}/\tilde{R}\tilde{T}),$$

where

$$\begin{pmatrix} a \\ b \end{pmatrix} = \begin{cases} a, & \tilde{x}_3 < \tilde{\phi}(\psi, \tilde{t}) \\ b, & \tilde{x}_3 > \tilde{\phi}(\psi, \tilde{t}). \end{cases}$$

Here $\tilde{T}$ denotes the temperature and $\tilde{Y}$ denotes the mass fraction of the deficient component of the reaction. The model assumes a phase change whereby the deficient component melts before reacting. The melting is assumed to occur at the surface

$$\tilde{x}_3 = \tilde{\phi}(\psi, \tilde{t}),$$

where $\tilde{\phi}$ is to be determined. Upon melting, the heat of fusion $\tilde{\gamma}$ is absorbed by the reactant, but is then released during the reaction process, as the final product is assumed to be in the solid phase. The heat of reaction $\tilde{\beta}$, is thus augmented by $\tilde{\gamma}$ beyond the melting surface. We also assume that the reaction rate is increased by a factor $\alpha > 1$ due to the increased surface to surface contact in the liquid phase. The other constants of the model are the thermal diffusivity $\tilde{\lambda}$, the activation energy $\tilde{E}$, the gas constant $\tilde{R}$, and the rate constant $\tilde{A}$. Melting is assumed to occur instantaneously at the melting temperature $\tilde{T}_m$, which is taken to be independent of the curvature of the melting surface. Across this surface the heat flux jumps by an amount proportional to $\tilde{Y}$, since only the reactant, and not the product, melts. Thus

$$\tilde{\lambda}\left[\frac{\partial \tilde{T}}{\partial n}\right]_{\tilde{x}_3=\tilde{\phi}} = -\tilde{\gamma}\tilde{Y}\tilde{V}_n,$$

where the unit normal to the melting surface, $\mathbf{n}$, is given by

$$\mathbf{n} = \frac{[-\tilde{\phi}_{x_1}, -\tilde{\phi}_{x_2}, 1]}{\sqrt{1+\tilde{\phi}_{x_1}^2+\tilde{\phi}_{x_2}^2}}.$$

$\tilde{V}_n$ is the normal velocity of the surface given by

$$\tilde{V}_n = \frac{\tilde{\phi}_{\tilde{t}}}{\sqrt{1+\tilde{\phi}_{\tilde{x}_1}^2+\tilde{\phi}_{\tilde{x}_2}^2}}, \tag{3.1}$$

and, for any quantity g,

$$[g]_{\tilde{x}_3=\tilde{\phi}} = g(\tilde{x}_3=\tilde{\phi}^+) - g(\tilde{x}_3=\tilde{\phi}^-),$$

denotes the jump in the quantity g across the surface. In addition, $\tilde{T}$ and $\tilde{Y}$ satisfy the boundary conditions

$$\tilde{Y}=\tilde{Y}_u, \qquad \tilde{T}=\tilde{T}_u \qquad \text{as} \quad \tilde{x}_3 \to -\infty$$
$$\tilde{Y}=0, \qquad \tilde{T}=\tilde{T}_a \qquad \text{as} \quad \tilde{x}_3 \to \infty,$$

where $\tilde{Y}_u$ and $\tilde{T}_u$ denote the unburned mass fraction and temperature, respectively, and $\tilde{T}_a$ denotes the adiabatic burned temperature. We note that the condition $\tilde{Y} \to 0$ $(\tilde{x}_3 \to \infty)$ is a consequence of the model and is not imposed as a boundary condition either in the analysis or in the computations. By considering the solution corresponding to a planar front moving with constant velocity from right to left, it is easy to show that

$$\tilde{T}_a = \tilde{T}_u + \tilde{\beta}\tilde{Y}_u.$$

We consider the problem for the case that burning occurs only on the surface of a cylinder $\tilde{x}_1^2+\tilde{x}_2^2=\tilde{R}_c^2$. The problem is nondimensionalized as follows: Let

$$Y=\frac{\tilde{Y}}{\tilde{Y}_u}, \qquad \theta=\frac{\tilde{T}-\tilde{T}_u}{\tilde{T}_a-\tilde{T}_u}, \qquad \phi=\frac{\tilde{\phi}\tilde{U}}{\tilde{\lambda}}, \qquad \gamma=\frac{\tilde{\gamma}}{\beta},$$

$$N=\tilde{E}/\tilde{R}\tilde{T}, \qquad \sigma=\frac{\tilde{T}_u}{\tilde{T}_a}, \qquad x_i=\frac{\tilde{x}_i\tilde{U}}{\tilde{\lambda}}, \qquad R_c=\frac{\tilde{R}_c\tilde{U}}{\tilde{\lambda}}, \qquad t=\tilde{t}\frac{\tilde{U}^2}{\tilde{\lambda}},$$

where $\tilde{U}$ is the adiabatic speed of a uniformly propagating planar reaction front. In addition, we introduce the moving coordinate system

$$z=x_3-\phi(\psi, t),$$

so that melting occurs at $z=0$. The independent variables are z and the azimuthal angle ψ. The equations of the model are

$$\begin{aligned}\theta_t&=\phi_t\theta_z+\nabla^2\theta+\Lambda Y\begin{pmatrix}1\\ \alpha(1+\gamma)\end{pmatrix}\exp\left(\frac{N(1-\sigma)(\theta-1)}{\sigma+(1-\sigma)\theta}\right)\\ Y_t&=\phi_t Y_z-\Lambda Y\begin{bmatrix}1\\ \alpha\end{bmatrix}\exp\left(\frac{N(1-\sigma)(\theta-1)}{\sigma+(1-\sigma)}\right),\end{aligned} \tag{3.2}$$

where

$$\Lambda=\Delta\left(\frac{(1+\gamma)}{\alpha(1-M)}+O\left(\frac{1}{\Delta}\right)\right), \qquad M=\left(1-\frac{(1+\gamma)}{\alpha}\right)e^{\Delta(\theta_m-1)}, \qquad \Delta=N(1-\sigma),$$

$$\nabla^2=\frac{1}{R_c^2}\frac{\partial^2}{\partial\psi^2}+\left[1+\frac{1}{R_c^2}\left(\frac{\partial\phi}{\partial\psi}\right)^2\right]\frac{\partial^2}{\partial z^2}-\frac{1}{R_c^2}\frac{\partial^2\phi}{\partial\psi^2}\frac{\partial}{\partial z}-\frac{2}{R_c^2}\frac{\partial\phi}{\partial\psi}\frac{\partial^2}{\partial\psi\,\partial z}. \tag{3.3}$$

We note that the Laplacian is no longer separable in these coordinates and that mixed derivatives occur. The solid flame eigenvalue Λ serves to fix the space and time scales of the problem. The first correction to Λ is derived in [18] and is employed in our model.

At the melting surface $z=0$, the heat of fusion is absorbed by the reactant. Thus

$$\phi_t=\frac{-1}{\gamma Y(0)}[\theta_z]\left(1+\frac{(\phi_\psi)^2}{R_c^2}\right) \tag{3.4}$$

and the boundary conditions are

$$\theta(t, z, \psi)\to 1(0) \qquad \text{as} \quad z\to\infty(-\infty) \tag{3.5a}$$

$$Y(t, z, \psi)\to 1 \qquad \text{as} \quad z\to-\infty \tag{3.5b}$$

$$\theta(t, 0, \psi)=\theta_m \tag{3.5c}$$

$$h(t, z, \psi)=h(t, z, \psi+2\pi), \tag{3.5d}$$

where h denotes T, Y, or ϕ.

In the limit of infinite activation energy the reaction zone shrinks to a surface, the solid flame front, across which the solution must satisfy certain jump conditions. A linear stability analysis of this model appeared in [18]. It was shown that solution branches depends on a parameter $\mu=\Delta/2(1-M)$. In our computations the activa-

tion energy is finite and thus there is a non-zero reaction even as $z \to -\infty$. Since in practice no significant reaction occurs ahead of the melting surface, the model described above is modified by multiplying the reaction term by a cutoff function

$$g(z) = 1 \qquad z \geqslant z_c$$
$$g(z) = 0 \qquad z < z_c,$$

where $z_c = -3$ in the present calculations. In addition, the boundary conditions (3.4a), (3.4b) are imposed at finite points z_L, z_r with

$$z_L = -z_r = -12.$$

This boundary is located sufficiently far from the reaction zone so that no sensitivity to the artificial boundary is observed.

The [illegible] of this [illegible] [illegible] multiple domain formulation for the problem. The solution is advanced separately on each of the domains $[z_L, 0]$ and $[0, z_R]$. The interface is the melting surface $z = 0$. Each domain is mapped onto the interval $[-1, 1]$ and the solution updated using the pseudo-spectral method. The location of the melting surface, $\phi(\psi)$, which enters into the coefficients as indicated in (3.3), is then updated using (3.4). The temporal difference scheme described below is designed to be as centered as possible so as to obtain the smallest possible temporal truncation error.

We now discuss certain aspects of the numerical method used to solve the system (3.2). Since the reaction zone occurs beyond the melting surface, i.e., $z > 0$, we introduce a mapping only in this region. The region of most rapid variation occurs very close to $z = 0$. The explicit mapping function is given in (2.8). The degree of stretching near the melting surface, $z = 0$, depends on the parameter α. In the computations, α is chosen for each value of ψ by the method described in Section 2. The axial derivative terms are computed using the Chebyshev pseudo-spectral method and the angular derivative terms are computed using a Fourier pseudo-spectral method.

The solution is advanced in time using a semi-implicit scheme. Terms involving the second derivative of the transformed axial coordinate are advanced implicitly with a backwards Euler predictor and a Crank–Nicolson corrector. All of the other terms are advanced using the modified Euler scheme. Specifically, assuming the model equation

$$U_t = A(t)\, U_{zz} + B(t)\, U_z + U_{\psi\psi},$$

the solution is advanced from time level n to time level $n+1$ as follows:

$$\frac{U^{n+1/2} - U^n}{0.5\, \Delta t} = A(t^n)\, U_{zz}^{n+1/2} + B(t^n)\, U_z^n + U_{\psi\psi}^n$$

$$\frac{U^{n+1} - U^n}{\Delta t} = A(t^{n+1/2})(U_{zz}^{n+1} + U_{zz}^n) + B(t^{n+1/2})\, U_z^{n+1/2} - U_{\psi\psi}^{n+1/2}.$$

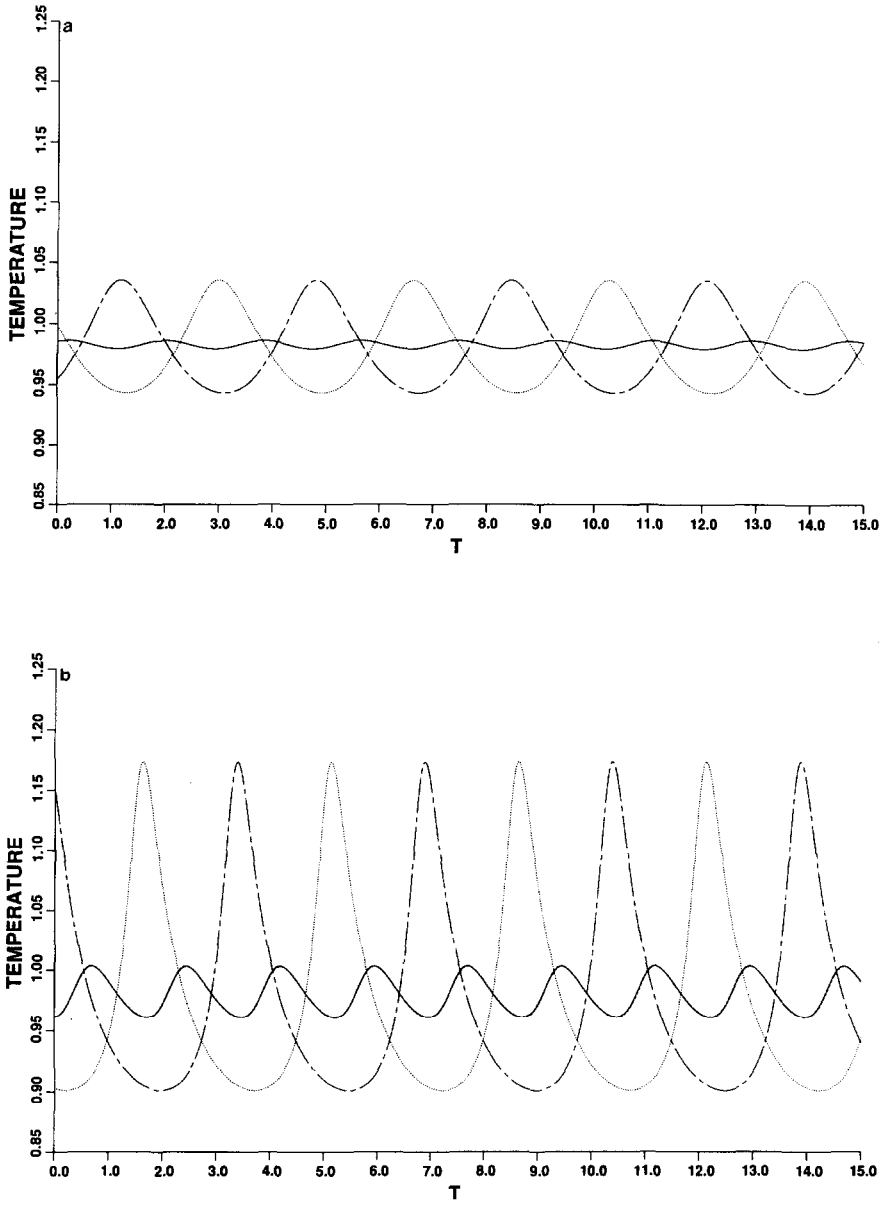

FIG. 1. (a) $\theta(t, z=0.4, \psi)$ for $\mu=4.0695$; ——— $\psi=0$; ... $\psi=\pi/2$; --- $\psi=\pi$; ———— $\psi=\frac{3}{2}\pi$. (b) $\theta(t, z=0.4, \psi)$ for $\mu=4.1613$; ——— $\psi=0$; ... $\psi=\pi/2$; --- $\psi=\pi$; ———— $\psi=\frac{3}{2}\pi$.

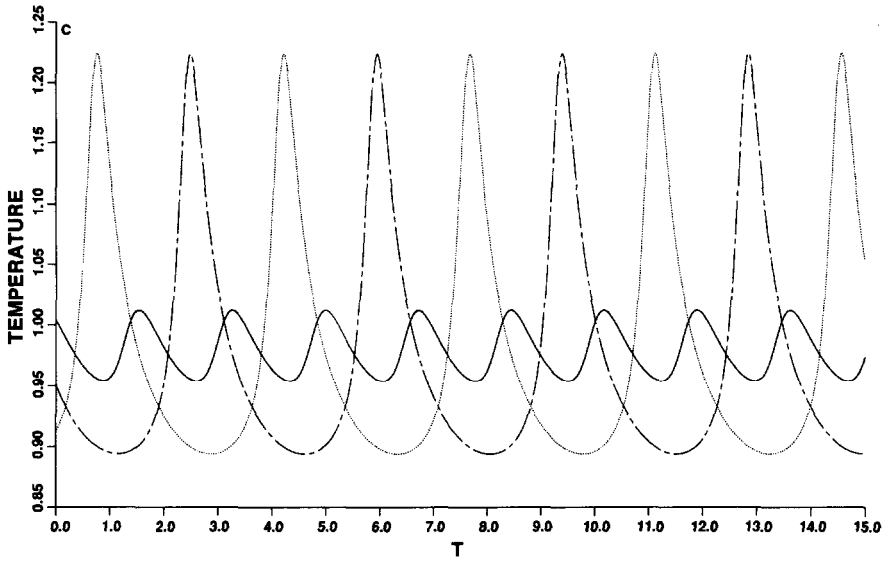

FIG. 1. (c) $\theta(t, z = 0.4, \psi)$ for $\mu = 4.2071$; ——— $\psi = 0$; ... $\psi = \pi/2$; --- $\psi = \pi$; ———— $\psi = \frac{3}{2}\pi$.

The functions $\phi_t(t, \psi)$ and $\phi(t, \psi)$ which appear in the coefficients (see (3.2) and (3.3)) are recomputed after the predictor step, i.e., at level $n + 1/2$ and then used in the corrector step. In the planar case the linear system associated with the implicit scheme is independent of time and the solution is updated by explicitly factoring the matrix associated with this linear system. In the present case the coefficients depend on both t and the angle ψ so that such a procedure is not practical. The implicit equations are solved iteratively using the minimum residual Richardson method as described in [9]. The system is preconditioned by using the finite difference discretization and solving the resulting tri-diagonal problem (see, for example, [8]). Typically the iteration converges to a relative residual of less than 10^{-5} in less than five iterations. We have found that stability can also be achieved by iterating for a fixed number of iterations. In our present implementation we employ one iteration for the predictor step in each domain and one iteration for the corrector step in the domain ahead of the melting surface. We employ two iterations for the corrector step in the domain behind the melting surface.

4. NUMERICAL RESULTS

We illustrate the method by exhibiting calculations of the solution along a standing wave branch. The numerical results will show a sinusoidal solution progressively sharpen into relaxation oscillations as the parameter μ is increased.

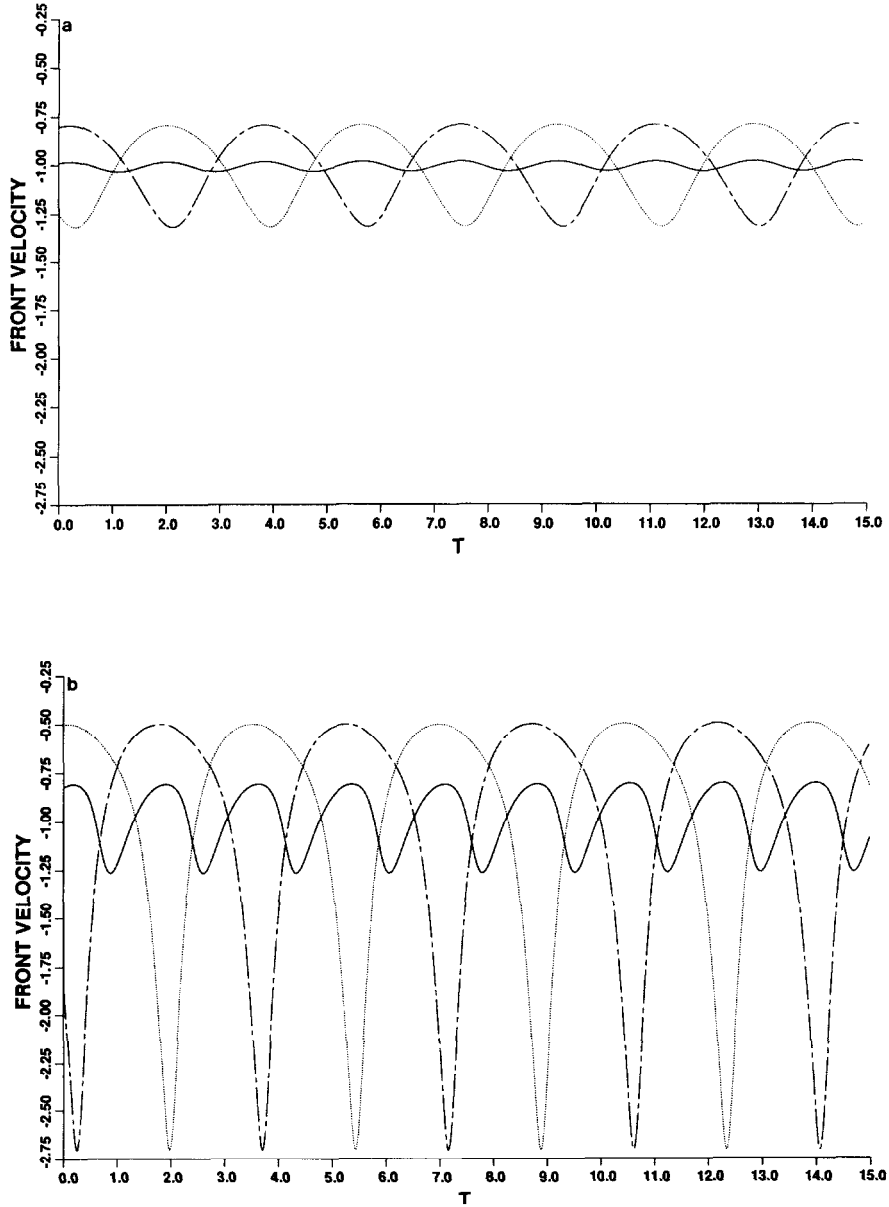

FIG. 2. (a) $V_n(t, \psi)$ for $\mu = 4.0695$; ——— $\psi = 0$; ... $\psi = \pi/2$; --- $\psi = \pi$; ———— $\psi = \frac{3}{2}\pi$.
(b) $V_n(t, \psi)$ for $\mu = 4.2071$; ——— $\psi = 0$; ... $\psi = \pi/2$; --- $\psi = \pi$; ———— $\psi = \frac{3}{2}\pi$.

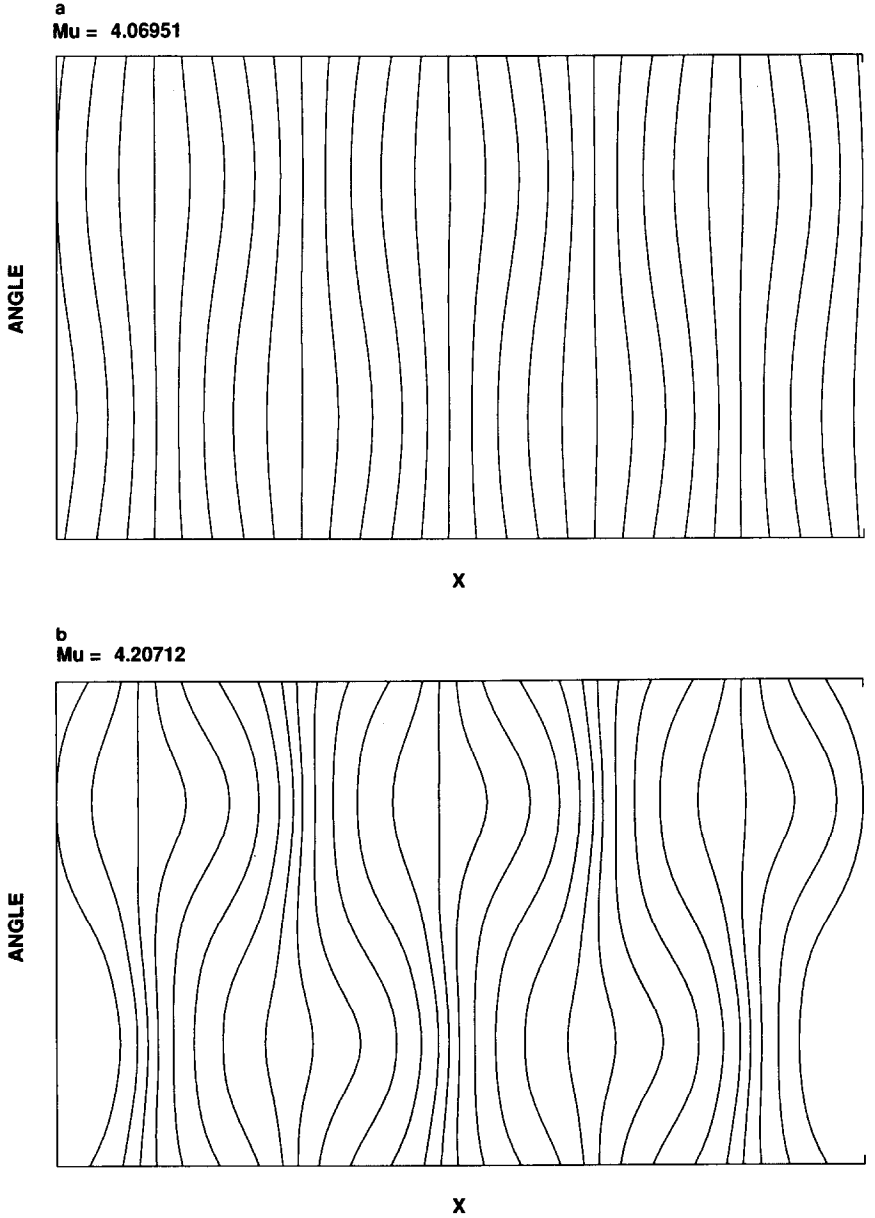

FIG. 3. (a) Location of melting surface at various times, $\mu = 4.0695$. (b) Location of melting surface t various times, $\mu = 4.2071$.

Beyond a certain point we find a transition to a branch of solutions which have a quasi-periodic time dependence. For the computations presented here the following parameters were held fixed: $N=50$, $\alpha=2.3$, $\gamma=0.37$, $\theta_m=0.8$. The bifurcation parameter μ was increased by decreasing the temperature ratio σ.

In Figs. 1a–c we illustrate the formation of relaxation oscillations by plotting $\theta(t, z=0.4, \psi)$ as a function of time for four different angles $\psi=0, \pi/2, \pi, 3\pi/2$. The value of μ is increased from 4.0695 (Fig. 1a) to 4.2071 (Fig. 1c). We observe that the solutions at $\psi=0$ and π are graphically indistinguishable. These angles correspond to the nulls of the standing wave. A small half period oscillation can be seen which grows as μ is increased. This oscillation, which is of much smaller amplitude than at the other angles, corresponds to a second-order term, as can be seen from the perturbation analysis of the solution in the vicinity of the standing wave bifurcation (see [19]).

In Figs. 2a–b we plot the normal velocity V_n (see (3.1)) as a function of time at the same angles. The values of μ are 4.0695 (Fig. 2a) and 4.2071 (Fig. 2b). In all cases the solution was obtained with a grid of 32 angular points and 61 axial points on either side of the melting surface. The solution was validated by computing on coarser grids. In both Figs. 1a–c and 2a–b we observe the progressive sharpening of the solution as μ is increased, indicating a transition from nearly sinusoidal behavior to relaxation oscillations. This sharpening of the pulsation in time is accompanied by an increase in the temperature at the spike and by a progressive sharpening of the spatial profile of the temperature at the time of the spike. In turn

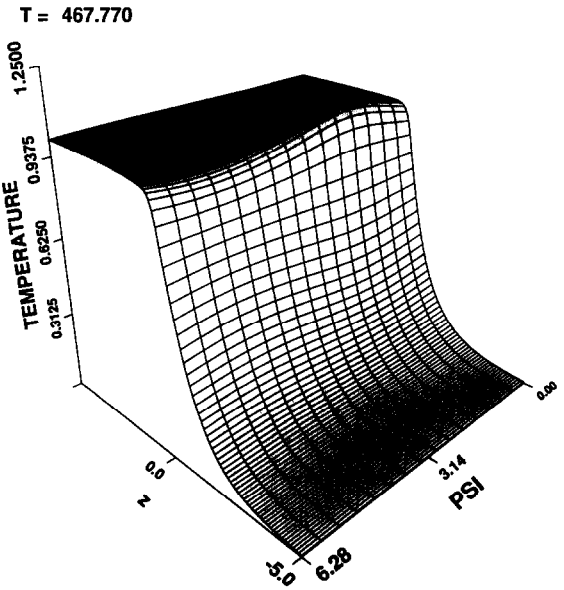

FIG. 4. $\theta(t, z, \psi)$ at a fixed time, $\mu=4.0695$.

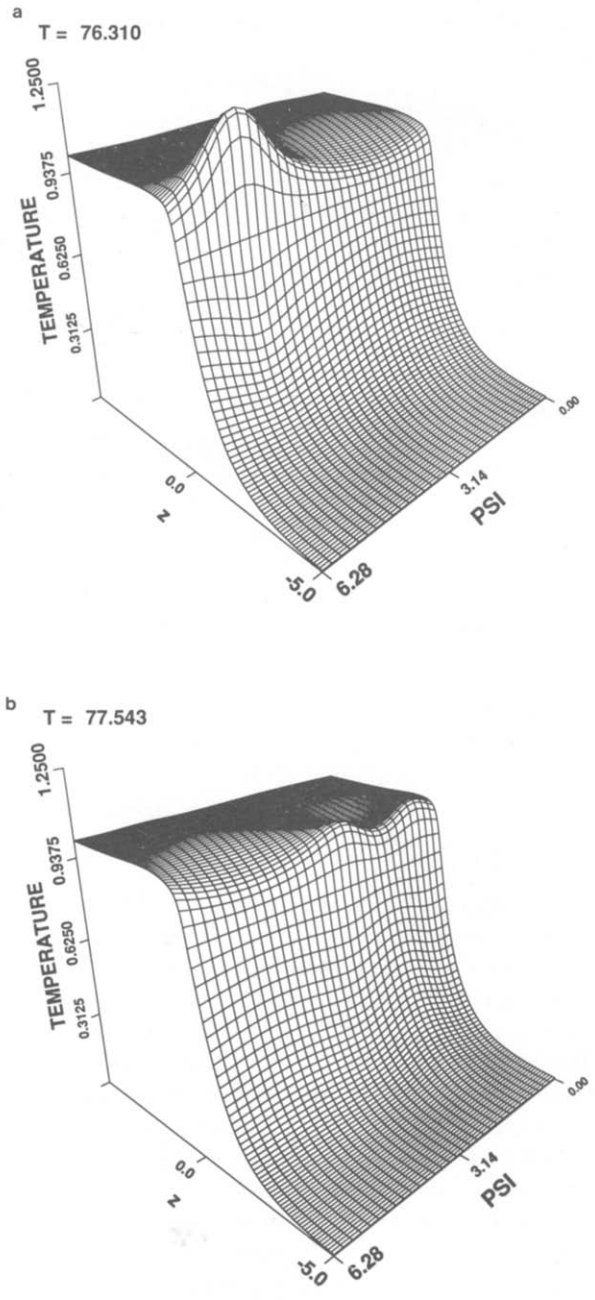

FIG. 5. (a) $\theta(t, z, \psi)$ at $t = t_1$, $\mu = 4.2071$. (b) $\theta(t, z, \psi)$ at $t = t_2$, $\mu = 4.2071$.

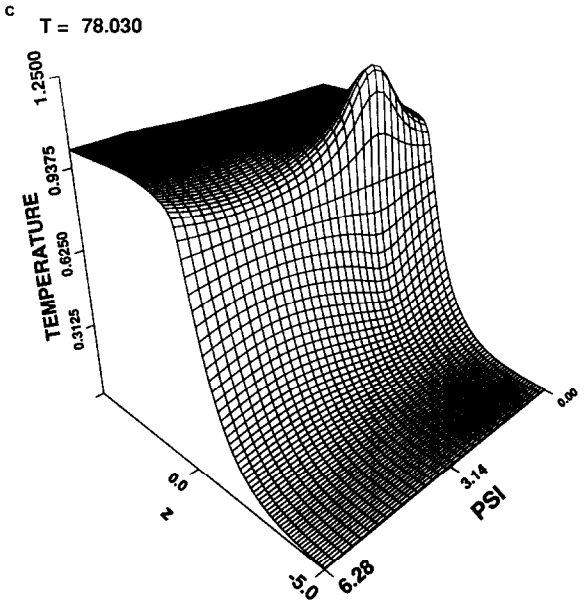

FIG. 5. (c) $\theta(t, z, \psi)$ at $t = t_3$, $\mu = 4.2071$.

there is a stronger angular dependence of the solution, requiring a greater degree of angular variability in the mapping function which is chosen as described above.

The increase in the angular variability of the solution is illustrated in Figs. 3a, b, where the location of the melting surface is plotted against the azimuthal angle ψ for different values of t for $\mu = 4.0695$ (Fig. 3a) and for $\mu = 4.2071$ (Fig. 3b). In order to illustrate the sharpening of the spatial profiles we exhibit perspective plots of the temperature field for different values of μ and for different times. In Fig. 4 we illustrate the temperature field for the case $\mu = 4.0695$ at a time close to a temperature spike at $\psi = \pi/2$. We observe both the nearly sinusoidal angular dependence and the relatively gradual variation with z. In Figs. 5a–c we plot the temperature field for the case $\mu = 4.2071$. It is apparent from the figures that both the temperature field and the location of the reaction zone have a stronger angular variational and there is a much more rapid axial variation in θ.

Upon further increasing μ we find that periodic solutions can no longer be computed and the solution undergoes a transition to apparently quasi-periodic behavior characterized by an oscillation comparable in frequency to that observed for lower values of μ, modulated by a lower frequency envelope. The variation in the amplitude of this envelope increases as μ is increased and appears to vanish as μ is decreased to a specific value, leading us to conjecture that the transition to quasi-periodicity occurs via bifurcation. In Fig. 6a we plot $\theta(t, z = 0.3, \psi)$ as a function of t for four different angles for the case $\mu = 4.3217$. The solution is exhibited over a

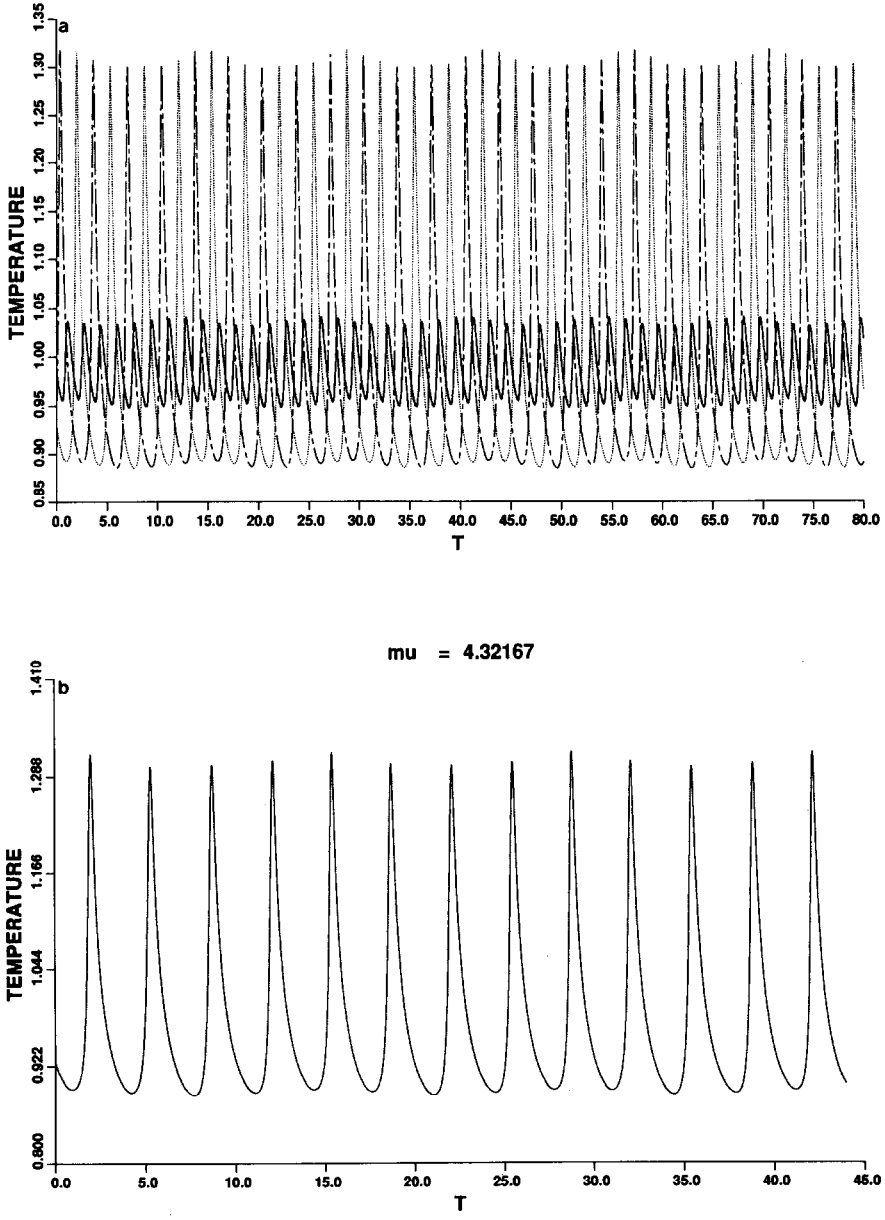

FIG. 6. (a) $\theta(t, z=0.3, \psi)$ for $\mu=4.3217$; ——— $\psi=0$; ... $\psi=\pi/2$; --- $\psi=\pi$; ——— $\psi=\frac{3}{2}\pi$. (b) $\theta(t, z=0.3, \pi/2)$ for $\mu=4.3217$.

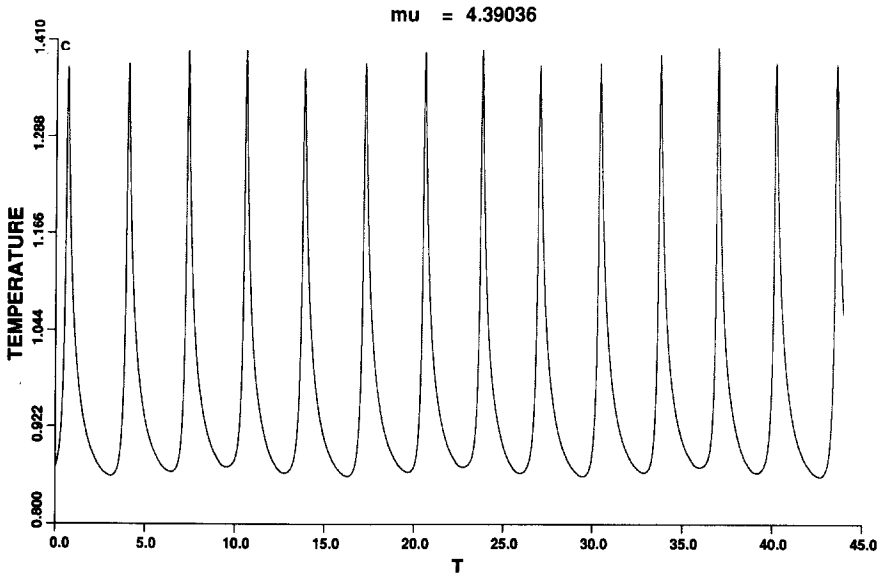

FIG. 6. (c) $\theta(t, z=0.3, \pi/2)$ for $\mu = 4.3904$.

long time interval so that the nature of the envelope is apparent. To illustrate the increase in the variation of the envelope with increasing μ, in Fig. 6b we plot the temperature at one angle for the case $\mu = 4.3217$. In Fig. 6c we plot the same quantity for the case $\mu = 4.3904$. The increase in the variation of the amplitude of the envelope is apparent.

Perspective plots of the temperature are shown in Fig. 7a ($\mu = 4.3217$) and Fig. 7b ($\mu = 4.3904$). These figures correspond to a value of t close to a temperature spike. The figures illustrate the rapid growth in the temperature spike and the increasing angular localization of the spike. The computations described above were obtained at the NMFECC and the NCSA.

In previous calculations with one-dimensional models it was found that the singly periodic solution underwent a transition to a doubly periodic behavior via a secondary bifurcation. This was shown both for a one-dimensional version of the melting model [1, 4, 5] and for a model which did not allow for melting [24]. In the melting model we observed a transition to chaotic behavior via intermittency, while in the nonmelting model we observed a transition to chaotic behavior via a period doubling sequence. In calculations of pulsating solutions of gaseous combustion models for Lewis numbers greater than one we also obtained a period doubling sequence. Quasi-periodic modes of propagation have been predicted for higher

the quasi-periodic behavior found in the non-axisymmetric problem appears to be a truly two-dimensional effect which is not present in one-dimensional models.

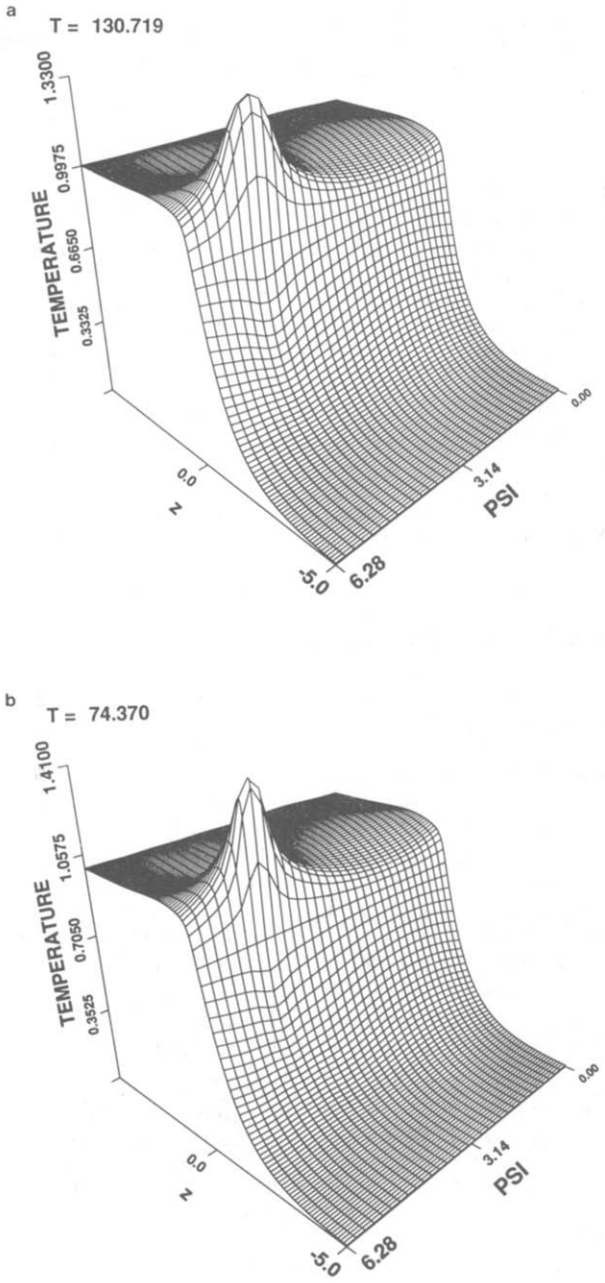

FIG. 7. (a) $\theta(t, z, \psi)$ at a fixed time; $\mu = 4.3217$. (b) $\theta(t, z, \psi)$ at a fixed time; $\mu = 4.3904$.

ACKNOWLEDGMENT

One of the authors (R.K.) would like to acknowledge the hospitality and stimulation of the Mathematics and Computer Science Division at Argonne National Laboratory where she was a summer student research participant.

REFERENCES

1. A. BAYLISS AND B. J. MATKOWSKY, *J. Comput. Phys.* **71**, 147 (1987).
2. A. BAYLISS AND B. J. MATKOWSKY, *Combustion and Plasma Synthesis of High-Temperature Materials*, edited by Z. A. Munir and J. B. Holt (VCH, New York, 1990), p. 61.
3. A. BAYLISS AND B. J. MATKOWSKY, *SIAM J. Appl. Math.* **50**, 437 (1990).
4. A. BAYLISS, B. J. MATKOWSKY, AND M. MINKOFF, *SIAM J. Appl. Math.* **49**, 1047 (1989).
5. A. BAYLISS, B. J. MATKOWSKY, AND M. MINKOFF, *SIAM J. Appl. Math.* **49**, 1421 (1989).
6. A. BAYLISS, B. J. MATKOWSKY, AND M. MINKOFF, *Lecture Notes in Physics, # 351 Numerical Combustion*, edited by A. Dervieux and B. Larrouturou (Springer-Verlag, New York, 1990), p. 187.
7. A. BAYLISS, D. GOTTLIEB, B. J. MATKOWSKY, AND M. MINKOFF, *J. Comput. Phys.* **81**, 421 (1989).
8. C. CANUTO, M. Y. HUSSAINI, A. QUARTERONI, AND T. A. ZANG, *Spectral Methods in Fluid Dynamics* (Springer-Verlag, New York, 1987).
9. C. CANUTO AND A. QUARTERONI, *J. Comput. Phys.* **60**, 315 (1985).
10. M. GARBEY, G. K. LEAF, H. G. KAPER, AND B. J. MATKOWSKY, *European J. Appl. Math.* **1**, 73 (1990).
11. D. GOTTLIEB, L. LUSTMAN, AND S. A. ORSZAG, *SIAM J. Sci. Stat. Comput.* **2**, 296 (1981).
12. D. GOTTLIEB AND S. A. ORSZAG, *Numerical Analysis of Spectral Methods: Theory and Applications*, C.B.M.S.-N.S.F. Regional Conference Series in Applied Mathematics (SIAM, Philadelphia, 1977).
13. G. H. GUILLARD AND R. PEYRET, *Comput. Methods Appl. Mech. Eng.* **66**, 17 (1988).
14. A. P. HARDT AND P. V. PHUNG, *Combust. Flame* **21**, 77 (1973).
15. J. B. HOLT, *Mat. Res. Soc. Bull.* **12**, 60 (1982).
16. YU. M. MAKSIMOV, A. G. MERZHANOV, A. T. PAK, AND M. N. KUCHKIN, Combustion, Explosion, and Shock Waves, **17**, 393 (1981).
17. YU. M. MAKSIMOV, A. T. PAK, G. B. LAVRENCHUK, YU. S. NAIBODORENKO, AND A. G. MERZHANOV, *Combust. Explosion Shock Waves* **15**, 415 (1979).
18. S. B. MARGOLIS, *SIAM J. Appl. Math.* **43**, 351 (1983).
19. S. B. MARGOLIS, H. G. KAPER, G. K. LEAF, AND B. J. MATKOWSKY, *Combust. Sci. Tech.* **53**, 289 (1987).
20. S. B. MARGOLIS AND B. J. MATKOWSKY, *SIAM J. Appl. Math.* **48**, 828 (1988).
21. B. J. MATKOWSKY AND G. I. SIVASHINSKY, *SIAM J. Appl. Math.* **35**, 456 (1978).
22. A. G. MERZHANOV, *Arch. Combust.* **1**, 23 (1981).
23. A. G. MERZHANOV, A. K. FILONENKO, AND I. P. BOROVINSKAYA, *Dokl. Phys. Chem.* **208**, 122 (1973).
24. K. G. SHKADINSKII, B. I. KHAIKIN, AND A. G. MERZHANOV, *Combust. Explosion Shock Waves* **7**, 15 (1971).
25. G. I. SIVASHINSKY, *SIAM J. Appl. Math.* **40**, 432 (1981).